

# Heat transfer from a negatively buoyant wall jet

K. KAPOOR and Y. JALURIA

Department of Mechanical and Aerospace Engineering, Rutgers—The State University of  
New Jersey, New Brunswick, NJ 08903, U.S.A.

(Received 3 November 1987 and in final form 26 August 1988)

**Abstract**—An experimental investigation has been carried out on the heat transfer characteristics of a turbulent, negatively buoyant, two-dimensional wall jet. The heat transfer to the surface from the jet, the discharge temperature of which is taken as greater than the surface temperature, is measured as a function of distance along the isothermal surface for several values of wall, jet and ambient temperatures. It is found that the total heat transfer rate to the isothermal vertical surface decreases with an increase in the mixed convection parameter. The effect of the surface temperature excess on the downward penetration of the jet and on the heat transfer rate is also investigated. Relevant correlating equations are derived.

## INTRODUCTION

BUOYANT jets are frequently encountered in nature as well as in industry. In nature, they are important in meteorological, oceanographic and environmental studies. The rejection of thermal energy and of chemical waste products to the atmosphere and to water bodies involves turbulent buoyant jets, such as the flows emerging from cooling towers or chimneys. Heat extraction and energy storage systems, such as those employed in solar energy utilization, are also often concerned with buoyant jet flows [1, 2].

Laminar buoyant jets have been analyzed in several investigations. These studies have clarified the basic mechanisms underlying such flows. For instance, Mollendorf and Gebhart [3] carried out a perturbation analysis for a vertical, laminar, axisymmetric jet, with a small amount of thermal buoyancy. The laminar buoyant jet flow, with small buoyancy effects, was also studied by Schneider and Potsch [4]. They obtained the first approximation to the effect of buoyancy on the flow by the method of matched asymptotic expansions, for  $0.5 < Pr < 1.5$ . Several other studies have obtained numerical and experimental results on laminar buoyant jets, as reviewed in ref. [5]. However, turbulent jets are of much greater practical interest and have, therefore, been studied much more extensively [1].

Very little work has been done on jets in which the buoyancy effects oppose the flow, such as heated jets discharged downward. Such flows arise in room fires and in mixed convection transport in enclosures. Energy extraction and heat rejection processes often lead to regions where the jet flow is opposed by the buoyancy force, see, for instance, refs. [6, 7].

The negatively buoyant, axisymmetric, jet has been studied experimentally and analytically, using integral models, as reported by Turner [8] and Seban *et al.* [9]. They found that the flow penetrates to a finite height,

where the vertical velocity drops to zero and flow reversal occurs, as expected. They also reported that the flow spreads outward horizontally as it approaches the location of flow reversal. The analysis did not consider the effect of the reverse flow on the jet, which is itself driven by an external momentum source. The idealized circumstances of a point-source jet with momentum and buoyancy input, but zero mass flux at the inlet, were considered in the analysis. Penetration distances were found to be close to the experimentally determined values. But the flow rates and the velocity and temperature distributions were not accurately predicted by the analysis.

In this paper, the rate of heat transfer to an isothermal vertical surface in the mixed convection circumstance of a negatively buoyant, turbulent, wall jet flowing adjacent to the surface is studied in detail. As mentioned above, this problem is of particular interest in room fires and in energy extraction and storage systems. The basic problem considered and the relevant flow configuration are discussed in detail later.

There are many practical situations where turbulent, negatively buoyant, wall flows arise [10]. For example, when the fire plume in an enclosure hits the ceiling, it spreads out and finally turns downward at the corners [11, 12]. At this stage, the flow of the wall jet is downward, whereas the buoyancy force is upward, since the flow is at a temperature higher than that of the surroundings. Similarly, heated flows rising adjacent to two walls may flow along the ceiling, meet at the top and be pushed downward, against the buoyancy force. This results in a negatively buoyant, two-dimensional, free jet. At a later stage in the growth of an enclosure fire, a hot upper layer is established above a relatively cooler lower layer. Then, a buoyancy-induced flow arises in the lower layer, adjacent to the wall which is usually hotter than the neighboring fluid. This flow becomes negatively buoyant as it penetrates into the upper layer, across the interface

## NOMENCLATURE

$A_0$	cross sectional area of the slot through which the jet is discharged	$\Delta T$	surface temperature excess over the ambient, $T_s - T_\infty$
$C_p$	specific heat of air at constant pressure	$T_0$	discharge temperature of the jet
$D$	width of the slot for jet discharge	$T_s$	temperature of the isothermal surface
$g$	magnitude of gravitational acceleration	$T_\infty$	temperature of the surroundings
$Gr$	Grashof number, $g\beta(T_0 - T_\infty)D^3/\nu^2$	$U_0$	discharge velocity of the jet
$h$	local surface heat transfer coefficient, $q''/\Delta T$	$V_{\max}$	maximum velocity in the upward natural convection flow adjacent to the plate for the case of $T_s > T_\infty$
$H$	height of the enclosure	$W$	width of the vertical plate
$k$	thermal conductivity of air	$x$	vertical coordinate distance, measured downward from the slot
$L$	height of the isothermal vertical surface	$X$	dimensionless vertical distance, $x/D$
$m_{\text{NC}}$	mass flow rate in the upward natural convection flow for the case when $T_s > T_\infty$	$y$	horizontal coordinate distance measured outward from the isothermal surface
$m_0$	mass flow rate discharged by jet per unit length of the slot	$Y$	dimensionless horizontal distance, $y/D$
$M_0$	momentum flow rate per unit slot length at the jet inlet	Greek symbols	
$Nu_D$	Nusselt number based on $D$ , $hD/k$	$\beta$	coefficient of thermal expansion of the fluid
$Nu_\delta$	Nusselt number based on $\delta_p$ , $h\delta_p/k$	$\nu$	kinematic viscosity of the fluid
$Pr$	Prandtl number	$\delta_p$	penetration distance of the jet, measured downward from the slot
$q''$	local heat transfer flux to the surface	$\delta_H$	vertical distance up to which heat is transferred from the jet to the isothermal plate
$Q$	total net heat transfer to the isothermal surface from the heated jet flow, $W \int_0^{\delta_p} q'' dx$	$\rho_0$	density of air at the jet discharge
$Q_{\text{IN}}$	total thermal energy input by the jet, $\rho_0 C_p U_0 A_0 (T_0 - T_\infty)$	$\theta$	dimensionless temperature, $(T - T_\infty)/(T_0 - T_\infty)$
$Re$	Reynolds number, $U_0 D/\nu$	$\theta_s$	dimensionless surface temperature, $(T_s - T_\infty)/(T_0 - T_\infty)$
$Ri$	Richardson number, $g\beta(T_0 - T_\infty)D/U_0^2 = Gr/Re^2$		
$T$	local fluid temperature		

separating the two regions [13, 14]. Negatively buoyant flows may also result due to the discharge of fluid at a temperature different from the ambient air and water media in which the transport occurs. Such flows arise, for instance, in energy extraction from a solar pond and heat rejection with jets inclined downward [7, 15].

A detailed experimental investigation to study the basic flow characteristics of negatively buoyant wall and free jets was carried out in ref. [16]. An insulated surface was employed in the study on wall jets. The penetration distance  $\delta_p$  was defined as the vertical distance up to which thermal effects penetrate, as indicated by a sharp increase in the temperature level as an array of thermocouples is moved upward starting from the ambient conditions far downstream. The penetration distance was measured and was found to be largely governed by the mixed convection, or buoyancy, parameter  $Gr/Re^2$ , which is also often termed the Richardson number,  $Ri$ . All these dimensionless parameters are based on the inlet conditions of the jet, as defined later. The net entrainment into the flow was also determined. It was found that as

$Gr/Re^2$  increases, resulting in larger buoyancy effects, the flow penetration decreases and a stronger reverse flow, in the direction of the buoyancy force, arises. The entrainment into the flow was found to increase with  $Gr/Re^2$ , over the range considered, as a result of this increased reverse flow at larger  $Gr/Re^2$ .

The effect of the thermal conditions at the wall, i.e. whether it is adiabatic, heated or cooled, on the behavior of negatively buoyant flows has not been investigated in detail. Also, since the wall was adiabatic in the experimental work of ref. [16], no data on the resulting heat transfer was obtained. The dependence of the wall flow on the thermal conditions at the surface and the heat transfer to the wall are of considerable importance in the modeling of the transient heating of the walls in enclosure fires and in the other practical cases mentioned earlier.

It is clear from the above review that the heat transfer characteristics of a turbulent, negatively buoyant, two-dimensional, wall jet are not available in the literature. The objective of the present study was to continue the work initiated in ref. [16] in order to determine the heat transfer from the wall jet to a

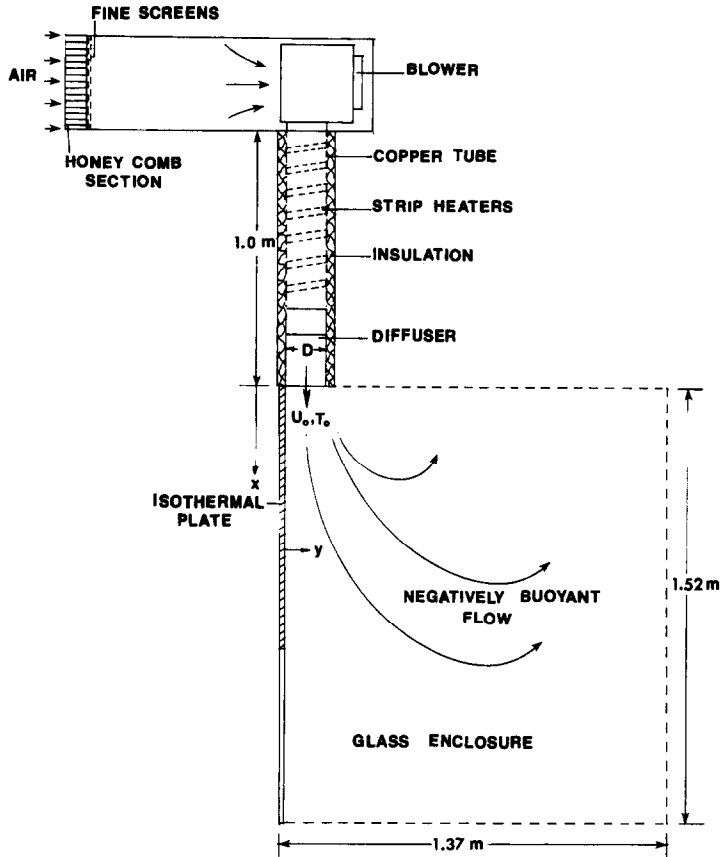


FIG. 1. Experimental arrangement for the study of a heated, two-dimensional downward discharged wall jet in an isothermal ambient medium.

cooled, isothermal surface, with the surface temperature  $T_s$  less than the jet discharge temperature  $T_0$ . Heat flux data have been obtained for several wall temperatures, varying  $Gr/Re^2$  from 0.05 to 1.05. The local heat flux distribution has been integrated over the surface up to  $\delta_p$ , the jet penetration distance, to obtain the total heat transfer from the jet to the surface. The effect of the wall temperature excess  $T_s - T_\infty$  on the penetration of the jet has also been studied. It is found that, for a given ambient temperature, the penetration distance  $\delta_p$  decreases as the surface temperature  $T_s$  increases, for  $Gr/Re^2 > 0.1$ . For smaller values of  $Gr/Re^2$ ,  $\delta_p$  was found to be essentially independent of the wall temperature excess. The effect of the upward natural convection boundary layer flow, which arises when the surface temperature  $T_s$  is greater than the ambient temperature  $T_\infty$ , is also studied and related to the basic transport mechanisms in the flow. Several very interesting and important trends are observed and considered in terms of the flow characteristics of a negatively buoyant wall jet.

## EXPERIMENT

### Experimental arrangement

Figure 1 shows a sketch of the experimental arrangement. A blower sends ambient air, over a fairly

wide range of flow rates, through a copper tube which is 5 cm in diameter and 1 m in length. The copper tube is heated by means of three fiberglass insulated strip heaters wrapped around it. The energy input to each of the heaters is varied by means of power controllers. A diffuser at the end of the copper tube helps in discharging the heated air as a two-dimensional jet. The width of the slot for discharge may be varied up to about 0.1 m. Several diffuser designs were considered in order to ensure a uniform two-dimensional flow at the exit. Temperature and velocity distributions at the diffuser exit were measured. These indicated that fairly uniform conditions, with variations of less than 10%, were obtained at the discharge location. The heat losses from the copper tube and from the diffuser to the environment were minimized by employing insulation made of foam and fiberglass.

The discharge velocity of the jet  $U_0$  could be varied from about  $0.3 \text{ m s}^{-1}$  at a slot width of 0.1 m to  $3.0 \text{ m s}^{-1}$  at a slot width of 0.01 m. The discharge temperature  $T_0$  could be raised to approximately  $150^\circ\text{C}$ . Thus, this arrangement could be used for studying fairly wide ranges of the governing parameters  $Re$  and  $Gr$ , based on the inlet conditions, as defined later. Values as high as around 3500 and  $10^6$  for  $Re$  and  $Gr$ , respectively, could be obtained. This study uses a slightly modified version of the system

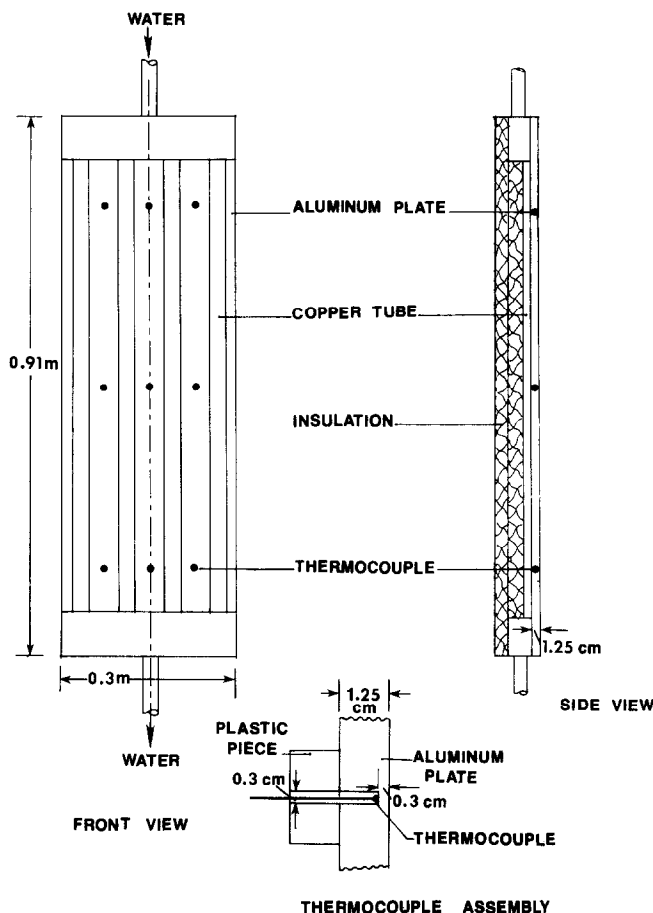


FIG. 2. Sketch of the arrangement used for generating an isothermal vertical surface.

described in ref. [16], which may be consulted for further details.

The heated, two-dimensional, air jet is discharged into a glass enclosure, 1.5 m high and  $1.37 \times 0.3$  m in cross section. The bottom of the enclosure is kept open in order to allow the wall jet flow to entrain ambient air from below or to flow out of the enclosure at a relatively small velocity, resulting in a negligible effect of the outflow on the negatively buoyant flows under investigation. The top and the far side of the enclosure are also kept open to allow a free exchange with the ambient medium. This arrangement, thus, simulates a wall jet in an extensive ambient medium and, as seen later, in a steady flow circumstance.

A water cooled aluminum plate was located vertically adjacent to the side wall of the enclosure over which the heated jet was discharged. The plate was 91.4 cm in height and 30 cm in width. The remaining portion of the side wall was insulated. The details of the plate design are shown in Fig. 2. Four rectangular copper tubes, each  $2.5 \times 1.2$  cm in cross section, run along the length of the plate. The tubes were kept flush with the plate surface and were bonded to it by soldering. It was ascertained that the contact between the two surfaces was good by means of temperature measurements. As can be seen from this figure, water

circulates over approximately 44% of the plate area. Water from an external tank enters at the top of the plate, with that emerging from this arrangement being allowed to drain into a sink. The temperature of the water entering the plate assembly could be maintained at a desired value by mixing hot and cold water streams from two separate tanks. Nine thermocouples were embedded in the plate to monitor the plate temperature. Details on the thermocouple assembly for plate temperature measurement are also shown in Fig. 2.

Several 0.3 cm diameter blind holes were drilled into the plate. Thermocouples, supported by 0.3 cm diameter glass tubes, were inserted into these holes. It was ensured that the thermocouple beads always touched the plate surface and that a good contact was maintained, so that the plate temperature was accurately obtained. Several similar arrangements have been used by the authors in the past and this background was used in the design of the arrangement. A 2 cm plastic cube was attached to the plate to support each glass tube. Finally, the plate was insulated at the back. It was found that the plate could be maintained at a constant temperature indefinitely. Also, it was confirmed by measurement that a fairly uniform temperature distribution was obtained at the

plate surface. The maximum temperature difference measured between any two surface thermocouples was around  $0.5^\circ\text{C}$ .

The temperature of the heated jet at the inlet was measured using a rake of five thermocouples. The rake was placed just below the slot through which the jet was discharged. The average of these five temperatures was taken as the jet temperature  $T_0$  in the experiments. The temperature was found to be very uniform, within  $\pm 2^\circ\text{C}$ , across the slot cross section. A DISA constant temperature hot-wire anemometer was employed for the velocity measurements. The hot wire was calibrated by measuring the frequency of the vortices behind a long cylinder [17]. The frequency in the wake allows the determination of air velocity across the cylinder. The velocity distribution at the discharge was again found to be very uniform, within a variation of less than 5%. The average of this distribution was taken to represent the jet discharge velocity  $U_0$ . Thus, fairly uniform velocity and temperature distributions were obtained at the discharge, and the measurements yielded the corresponding values of the jet discharge velocity  $U_0$  and temperature  $T_0$ . The intensity of the turbulence was found to be less than 5%, as was the intensity of the thermal fluctuations.

The heat transfer to the plate was measured by means of microfoil heat flow sensors (RdF Type 20472-3). Each of the heat flow sensors was  $15 \times 6$  mm in cross section and 1 mm in thickness. They could easily be attached to the plate surface. The electric output (in mV) from each heat flow sensor was converted into the corresponding heat flux  $q''$  (in  $\text{W m}^{-2}$ ) with the help of individual calibration curves supplied by the manufacturer. The calibration was also checked for accuracy, using electrically heated foils. These heat flow sensors were found to be highly sensitive and accurate. They covered the entire range of heat flux obtained in the experiments. Eighteen such heat flow sensors were attached, at a regular interval of 5 cm, along the centerline of the plate. The sensors were also moved around to confirm the two-dimensionality of the transport process.

The voltage signals from the hot-wire anemometer, thermocouples and the heat flow sensors were fed into a data acquisition system. The signal was also recorded on a strip chart recorder. The fluctuating component was generally found to be small, being less than 10% of the mean temperature and heat flux values. Thus, the mean values, which are of main interest in this study, were obtained easily. The experimental arrangement simulates a negatively buoyant wall jet in an extensive isothermal environment. Considerable care had to be taken to ensure that a high level of repeatability, within 5–10%, was maintained and that accurate measurements of the temperature field and of the heat transfer rate were obtained.

## RESULTS AND DISCUSSION

The width  $D$  of the long slot discharging the jet is generally taken as the characteristic dimension for a

jet in an extensive environment [9, 10]. Then, the dimensionless parameters that govern the flow are the Reynolds number  $Re$ , the Grashof number  $Gr$  and the Richardson number  $Ri$ , which is also often known as the mixed convection parameter,  $Gr/Re^2$ . The heat transfer at the wall may be presented in terms of the Nusselt number  $Nu_D$  [10]. These dimensionless quantities are defined for a negatively buoyant wall jet in an extensive isothermal medium at temperature  $T_\infty$  as

$$Re = \frac{U_0 D}{\nu}, \quad Gr = \frac{g\beta(T_0 - T_\infty)D^3}{\nu^2} \quad (1)$$

$$Ri = \frac{g\beta(T_0 - T_\infty)D}{U_0^2}, \quad Nu_D = \frac{hD}{k} \quad (2)$$

where  $U_0$  and  $T_0$  are the velocity and temperature at the discharge of the jet,  $g$  the magnitude of the gravitational acceleration,  $\beta$  the coefficient of thermal expansion of the fluid,  $h$  the local convective heat transfer coefficient, given by  $h = q''/\Delta T$  where  $q''$  is the local heat flux input at the surface and  $\Delta T$  the surface temperature excess over the ambient, and  $\nu$  the kinematic viscosity of air at the discharge temperature  $T_0$ .

It must be mentioned that the above dimensionless parameters are obtained when the governing equations and the boundary conditions are non-dimensionalized with  $U_0$ ,  $T_0$  and  $D$  as the characteristic quantities [10]. Another Nusselt number,  $Nu_\delta$ , based on the penetration distance  $\delta_p$ , is also defined as

$$Nu_\delta = \frac{h\delta_p}{k} \quad (3)$$

where  $\delta_p$  is the vertical penetration depth of the thermal effects in the wall jet flow, as defined quantitatively in terms of the thermal field later. If the average heat transfer coefficient  $\bar{h}$  is employed instead of  $h$  in equations (2) and (3), the average Nusselt number  $Nu_D$  or  $Nu_\delta$  is obtained. The dimensionless local temperature  $\theta$  and the dimensionless surface temperature  $\theta_s$  are defined as

$$\theta = \frac{T - T_\infty}{T_0 - T_\infty}, \quad \theta_s = \frac{T_s - T_\infty}{T_0 - T_\infty} \quad (4)$$

where  $T$  is the local temperature in the flow and  $T_s$  the surface temperature.

The data consist mainly of the temperature distributions in the wall jet flow and of the local heat flux measurements along the isothermal surface for different values of the physical variables such as temperatures and flow rates. Results on the flow field were given in ref. [16]. Detailed measurements were taken here for several values of the wall temperature  $\theta_s$ . The mixed convection parameter  $Ri = Gr/Re^2$  was varied from about 0.05 to 1.05 in the experiments, by varying the discharge velocity  $U_0$ , slot width  $D$  and temperature  $T_0$ . However, for convenience, the slot width

Table 1. Physical variables employed in the experiments

Fig. no.	$T_0$ (°C)	$U_0$ (m s <sup>-1</sup> )	$T_s$ (°C)	$Gr \times 10^{-6}$	$Re \times 10^{-3}$	$Gr/Re^2$
3	86.2	0.940	38.0	9.64	28.0	0.123
	101.1	0.702	38.0	9.94	19.4	0.263
4	Varied (75.0–153.0)	Varied (0.43–1.07)	Varied (22.0–48.0)	9.14–9.50	9.6–33.8	0.08–1.04
5	101.4	0.701	22.0	9.95	19.4	0.265
6	122.4	0.578	38.0	9.83	14.5	0.470
7	122.4	0.578	Varied (22.0–48.0)	9.83	14.5	0.470
8–10	Varied (75.0–153.0)	Varied (0.43–1.07)	Varied (22.0–48.0)	9.14–9.49	9.6–33.8	0.08–1.04

$D = 0.065$  m and  $T_\infty = 25.0^\circ\text{C}$ .

$D$  is held constant at 6.5 cm for the results presented here. The effects of varying  $U_0$ ,  $T_0$  and  $D$  were all found to be well correlated in terms of  $Ri$ , as found in ref. [16]. Also, even though  $D$  is used as a characteristic dimension here, results may be presented in terms of the discharge flow rate, per unit slot length,  $m_0$ , momentum inflow rate and energy input rate [5, 8]. For instance,  $m_0^2/\rho_0 M_0$ , where  $M_0$  is the momentum input per unit slot length at the jet discharge, may be used as a characteristic dimension instead of  $D$ . Table 1 gives the physical variables employed for the results presented here.

Figure 3 shows typical vertical temperature profiles

taken at  $y/D = 0.154$  for the negatively buoyant jet flow at  $Ri = Gr/Re^2 = 0.123$  and 0.263. This value of  $y$  corresponds closely to the location of maximum temperature in the wall jet. Thus, Fig. 3 indicates the decay of the maximum temperature in the downward wall jet flow with vertical distance away from the jet inlet,  $x = 0$ . It is seen that the maximum temperature level decreases sharply vertically downward up to a certain distance. This is followed by a more gradual decrease, with the temperature finally becoming equal to that of the surroundings, as expected. The penetration distance  $\delta_p$  is defined to represent the vertical penetration of thermal effects in the flow. This pen-

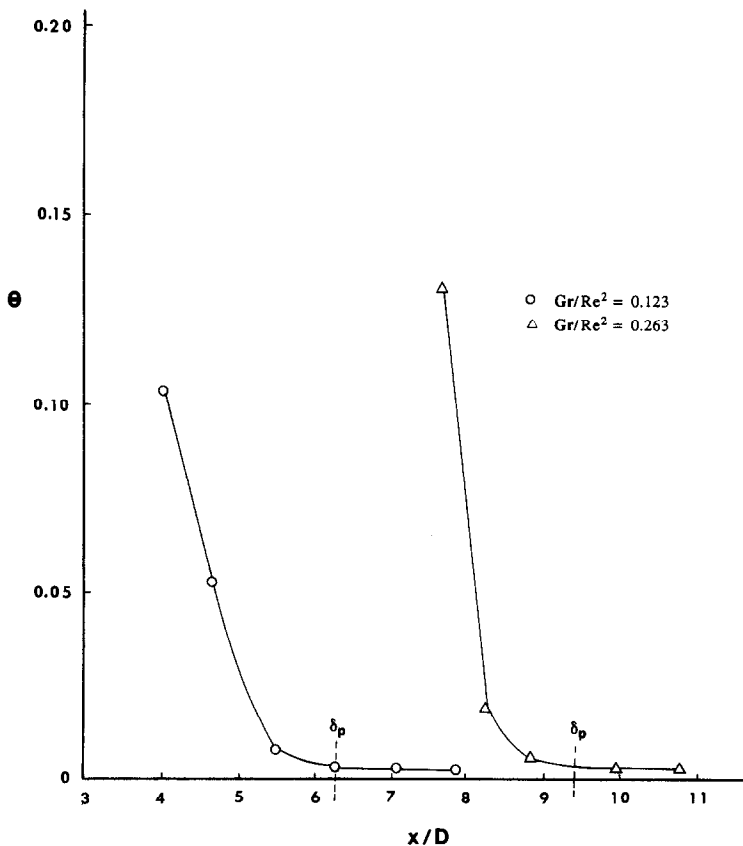


FIG. 3. Typical vertical temperature profiles in the negatively buoyant wall jet flow at  $Gr/Re^2 = 0.123$  and 0.263,  $y/D = 0.154$  and  $\Delta T = 13^\circ\text{C}$ .

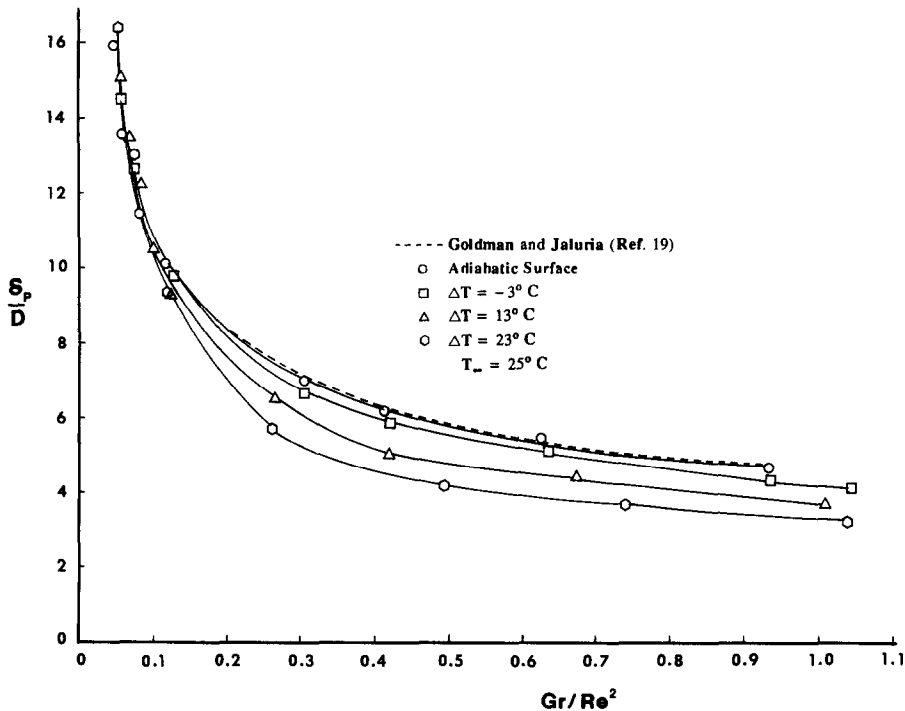


FIG. 4. Variation of the penetration distance  $\delta_p$  with the mixed convection parameter  $Gr/Re^2$  for adiabatic and three isothermal wall conditions.

etration is indicated quantitatively by a sharp rise in the maximum local temperature level as one proceeds from the bottom to the top of the tank. A unique value of  $\delta_p$  for given inlet conditions was obtained with this definition. It was found that this location was quite sharply defined, within 1–2 cm, and is marked in the figure. A similar behavior has been observed earlier [16] and repeatability to within 5–10% of the values of  $\delta_p$  was obtained in separate experiments. The vertical temperature distribution shown in Fig. 3 is important in the understanding of the basic heat transfer and fluid flow characteristics of a negatively buoyant wall jet and will be referred to later.

In fact,  $\delta_p$  may also be defined as the vertical distance by which the maximum temperature excess  $T - T_\infty$  in the downward flow has dropped to, say, 1% of the inlet temperature excess  $T_0 - T_\infty$ . However, such a definition is arbitrary and was found to yield poor repeatability because of the relatively gradual temperature variation far downstream of the discharge. A definition of  $\delta_p$  based on the temperature profiles shown in Fig. 3 and on a sharp deviation in the distribution due to thermal effects, as  $x$  is reduced from large values was found to be appropriate, well defined and repeatable.

The variation of the penetration distance  $\delta_p$  with the mixed convection parameter  $Gr/Re^2$  for adiabatic and isothermal wall conditions, considering three different typical values of  $\Delta T$ , the wall temperature excess over the ambient temperature  $T_\infty$ , are shown in Fig. 4, with  $\delta_p$  normalized by  $D$ . As can be seen from this figure, the penetration distance  $\delta_p$  for an adiabatic wall condition is very close to that reported

earlier [16]. It is also observed that penetration is essentially the same for various wall temperatures if  $Gr/Re^2 < 0.1$ . However, for  $Gr/Re^2 > 0.1$ , the penetration distance was found to vary significantly with the wall temperature excess  $\Delta T$ . For a given value of  $Gr/Re^2$ , the jet penetration distance  $\delta_p$  was found to be smaller for a larger value of the wall temperature excess  $\Delta T$ . This is an expected trend, since a larger wall temperature excess  $\Delta T$  results in a smaller heat transfer to the wall. This gives rise to a larger buoyancy effect, which retards the flow more rapidly, resulting in smaller  $\delta_p$ . Similar trends were observed for other wall temperatures considered in this study.

The effect of the wall temperature on the penetration of the jet also depends on whether  $T_s$  is larger or smaller than  $T_\infty$ . When the surface temperature  $T_s$  is higher than that of the surroundings, the surface induces a buoyancy driven flow which originates at the bottom edge of the surface and proceeds vertically upward. This convective mass flow opposes the jet flow which is discharged at the top. The calculations for the resulting laminar natural convection flow in air [10] for a surface temperature of  $48^\circ\text{C}$  with  $T_\infty = 25^\circ\text{C}$ , at the locations where the jet was found to reverse direction, show that the maximum natural convection velocity  $V_{\max}$  is 0.087 and  $0.345 \text{ m s}^{-1}$ , for  $Gr/Re^2 = 0.1$  and 1.05, respectively. Thus, for air,  $V_{\max}/U_0$  varies from 0.19 at  $Gr/Re^2 = 0.1$  to 0.8 at  $Gr/Re^2 = 1.05$ . However, the ratio of the mass flow  $m_{\text{NC}}$  in the natural convection boundary layer to the discharged jet mass flow  $m_0$ ,  $m_{\text{NC}}/m_0$ , varies from 0.004 at  $Gr/Re^2 = 0.1$  to 0.27 at  $Gr/Re^2 = 1.05$ . These calculations indicate that the natural convective flow

may have a considerable effect on the reversal of the jet flow for  $Gr/Re^2 > 0.1$ , if the plate temperature  $T_s$  is much larger than  $T_\infty$ . However, in many problems of practical interest, such as the enclosure fire at the early stages of the fire,  $T_s$  is quite close to  $T_\infty$  and the upward natural convection flow is negligible. This study has considered the circumstances of both negligible and significant natural convection boundary layer flow along the plate.

The variation of the non-dimensional penetration distance  $\delta_p/D$  as a function of  $Gr/Re^2$  over the range  $0 < Gr/Re^2 < 1.0$  may be expressed in terms of appropriate correlations. These were derived from the data obtained for  $-5^\circ\text{C} < \Delta T < 30^\circ\text{C}$  ( $0.08 < \theta_s < 0.6$ ) and are given as:

for the adiabatic wall condition

$$\frac{\delta_p}{D} = 4.5[Gr/Re^2]^{-0.402}; \quad (5)$$

for the isothermal wall condition

$$\frac{\delta_p}{D} = (4.1 - 5.9\theta_s)(Gr/Re^2)^{-(0.4 + 0.9\theta_s)}; \quad (6)$$

where  $\Delta T = T_s - T_\infty$  and  $\theta_s = (T_s - T_\infty)/(T_0 - T_\infty)$ . These correlations were found to represent the experimental data closely. The correlation coefficients were about 0.99, indicating this close agreement. In these correlations, the effect of the inlet conditions of the jet is largely represented by  $Gr/Re^2$  and that of the wall temperature by  $\theta_s$ . The penetration is also seen to be larger for the adiabatic condition, as compared to the isothermal cases, over the ranges considered. This is an expected result, since the buoyancy effect is the largest in this case because of negligible energy loss to the insulated surface.

Figure 5 shows the variation of the dimensionless local heat transfer rate, in terms of the local Nusselt number  $Nu_D$ , along the surface for  $Gr/Re^2 = 0.265$  and  $\Delta T = -3^\circ\text{C}$  ( $\theta_s = -0.039$ ). It is seen that the local heat transfer rate decreases sharply along the plate up to  $x/D \approx 5.5$  and then remains essentially constant, at a fairly small value over the remaining portion of the surface. Thus, the local heat transfer to the surface does not become zero even after the jet reverses its direction. This is obviously due to the fact that the ambient temperature  $T_\infty$  is slightly higher than the wall temperature  $T_s$ , i.e.  $\theta_s$  is negative. This temperature difference results in heat transfer by natural convection to the surface. The penetration distance  $\delta_p$ , obtained from the vertical temperature distributions for these experimental conditions, has also been marked in the figure. It is interesting to note that the jet loses most of its thermal energy to the surface within a fairly short distance from the slot at these conditions. This distance represents the region over which the heated jet loses thermal energy to the plate. It is denoted by  $\delta_H$  and is also shown in Fig. 5. Typically,  $\delta_H$  was found to be 70–80% of the corresponding penetration distance  $\delta_p$  in the present

experiments. Thus, even though the thermal effects, in terms of temperature disturbances and maximum temperature excess over the ambient, penetrate to a distance  $\delta_p$ , the heat flux becomes negligibly small upstream of the location of flow reversal. Such trends have been observed in other convective flows as well, such as deviation from the laminar behavior in transition to turbulence [10].

Figure 6 shows the variation of the local Nusselt number  $Nu_D$  with the vertical distance  $x/D$  for wall temperature excess  $\Delta T = 13^\circ\text{C}$  ( $\theta_s = 0.133$ ). The basic trends are similar to those observed in Fig. 5, except that the local heat transfer rate becomes negative after a certain distance, implying heat transfer from the surface to the flow. This distance is  $\delta_H$ , as defined earlier, and indicates the region over which the surface gains energy from the flow. Some of the corresponding values of  $\delta_H$  may also be marked on the respective vertical temperature profiles in Fig. 3. It was found that  $\delta_H$  indicates the vertical location where the local jet temperature near the surface becomes essentially equal to the surface temperature  $T_s$ . Thus, from Fig. 6, it is seen that the negatively buoyant jet loses energy to the surface up to a distance  $\delta_H$  where the local temperature level near the surface in the jet flow becomes essentially equal to the surface temperature. The temperature in the jet flow from  $\delta_H$  to  $\delta_p$  is actually lower than the surface temperature for positive  $\theta_s$ . Consequently, heat is transferred from the isothermal surface to the jet flow in this region. This is shown as  $Q_-$  in Figs. 6 and 7 and has been subtracted from  $Q_+$ , also shown in the figure, to obtain the total net energy transfer to the plate  $Q$ .

The distribution of the local Nusselt number  $Nu_D$  along the isothermal surface, at a constant value of  $Gr/Re^2$  and for the three plate temperatures, is shown in Fig. 7. The corresponding penetration distances  $\delta_p$  have also been marked in the figure. Obviously, the trends are the same as those observed in Figs. 5 and 6. This figure, therefore, indicates the effect of the plate temperature  $\theta_s$  on the heat transfer rate at a given value of  $Gr/Re^2$ . Other wall temperatures and different values of  $Gr/Re^2$  were also considered and similar trends observed.

The variation of the non-dimensional distance for heat loss,  $\delta_H/D$ , with  $Gr/Re^2$ , for different wall temperatures, is shown in Fig. 8. It is seen that  $\delta_H$  decreases as  $Gr/Re^2$  increases, which is expected since a larger value of  $Gr/Re^2$  implies larger buoyancy effects and thus a shorter penetration distance [16]. These results may be compared with the corresponding results for the penetration distance  $\delta_p$  shown in Fig. 4. It is seen from Fig. 8 that  $\delta_H$  is different for different wall temperature excess values, even for  $Gr/Re^2$  less than 0.1. This was not found to be the case for the penetration distance  $\delta_p$  (Fig. 4). From these results, it may be concluded that for small values of  $Gr/Re^2$ , even though the penetration distance  $\delta_p$  is essentially unaffected by the wall temperature excess  $\Delta T$ ,  $\delta_H$  does vary significantly



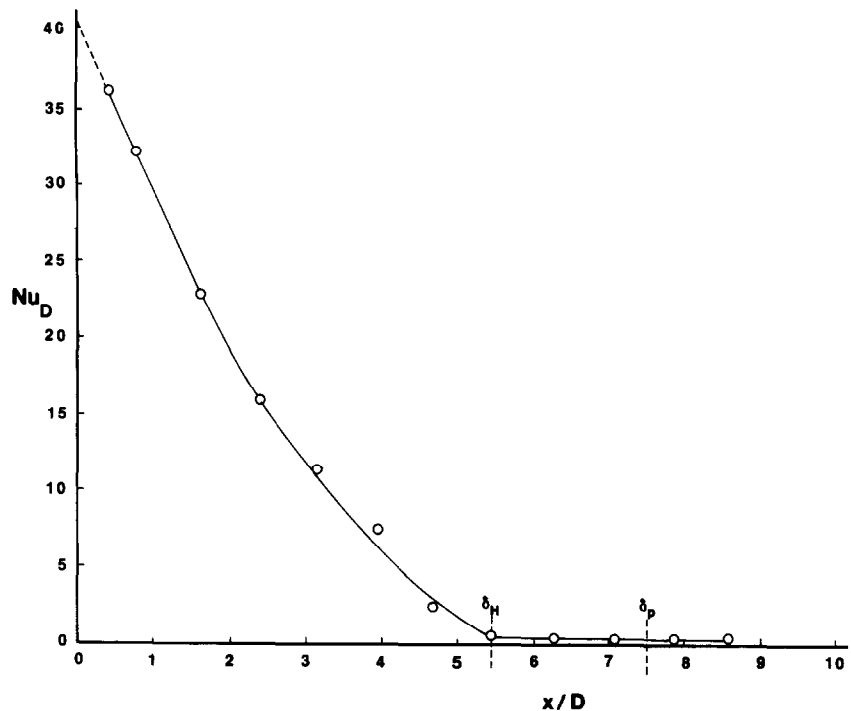


FIG. 5. Local Nusselt number  $Nu_D$  distribution along the surface for  $Gr/Re^2 = 0.265$  at a surface temperature  $T_s$  which is  $3^\circ\text{C}$  less than the ambient temperature  $T_\infty$  ( $\theta_s = -0.039$ ).

with  $\Delta T$ . For large values of  $Gr/Re^2$ , both the penetration distance  $\delta_p$  and the heat loss distance  $\delta_H$  were found to be significantly dependent on the plate temperature excess  $\Delta T$ .

For various values of  $Gr/Re^2$  and different wall conditions, the local heat flux  $q''$  was obtained as a

function of distance  $x$  along the plate. Then, the total net heat transfer  $Q$  to the plate by the jet was obtained by integrating  $q''$  up to the corresponding penetration distance  $\delta_p$  and multiplying the result by the plate width  $W$ . Thus, for wall temperatures higher than  $T_\infty$ , the thermal energy transferred by the isothermal plate

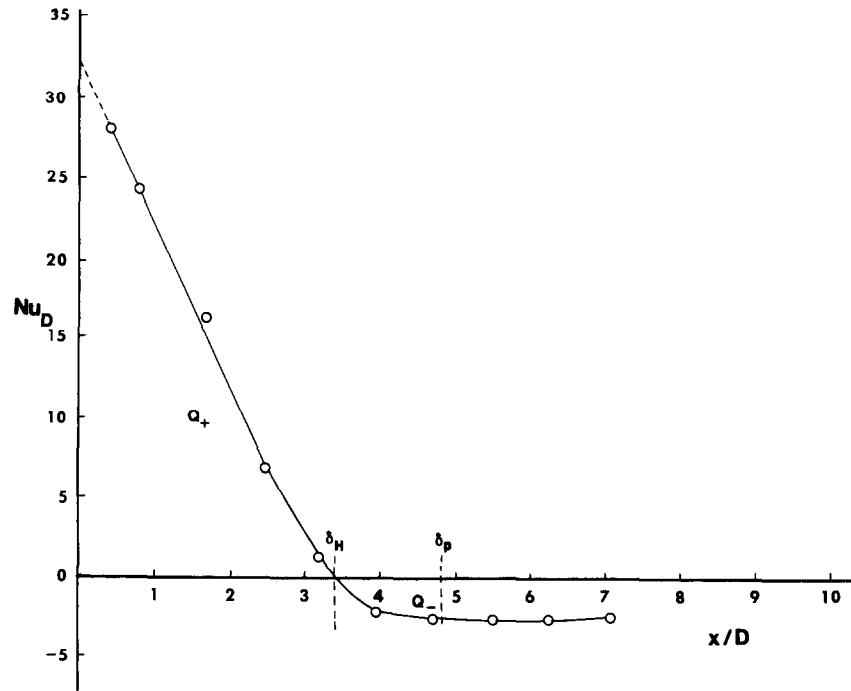


FIG. 6. Local Nusselt number distribution along the surface for  $Gr/Re^2 = 0.470$  and a surface temperature excess over the ambient  $\Delta T = 13^\circ\text{C}$  ( $\theta_s = 0.133$ ).

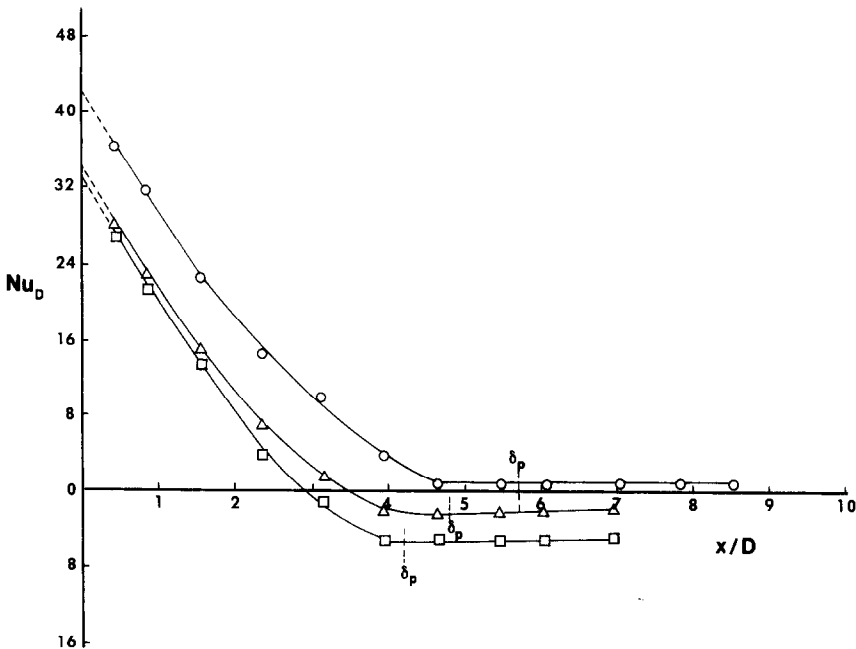


FIG. 7. Variation of the local Nusselt number  $Nu_D$  along the isothermal surface at  $Gr/Re^2 = 0.47$  for  $\theta_s$  values of: (a)  $\circ$ ,  $-0.039$ ; (b)  $\triangle$ ,  $0.133$ ; (c)  $\square$ ,  $0.236$ .

to the jet flow,  $Q_-$ , was subtracted from the thermal energy transferred to the plate by the jet  $Q_+$  to obtain  $Q$  ( $Q = Q_+ - Q_-$ ). This gives the net energy transferred by the jet to the wall. The natural convection transport beyond  $\delta_p$  is not considered in this calculation.

The total net heat transfer  $Q$  to the isothermal plate by the jet for the three plate temperature excess values considered earlier is shown as a function of  $Gr/Re^2$  in

Fig. 9. It is seen that for a  $\Delta T$  of  $-3^\circ\text{C}$ ,  $Q$  decreases sharply up to  $Gr/Re^2 \approx 0.25$ . This is followed by a gradual decrease up to  $Gr/Re^2 = 1.05$ . For plate temperature excesses of  $13$  and  $23^\circ\text{C}$ , the variation in  $Q$  with  $Gr/Re^2$  is found to be much smaller. In this figure,  $Q$  is nondimensionalized by the total energy input by the jet  $Q_{IN}$  which is calculated as follows:

$$Q_{IN} = \rho_0 C_p U_0 A_0 (T_0 - T_\infty). \tag{7}$$

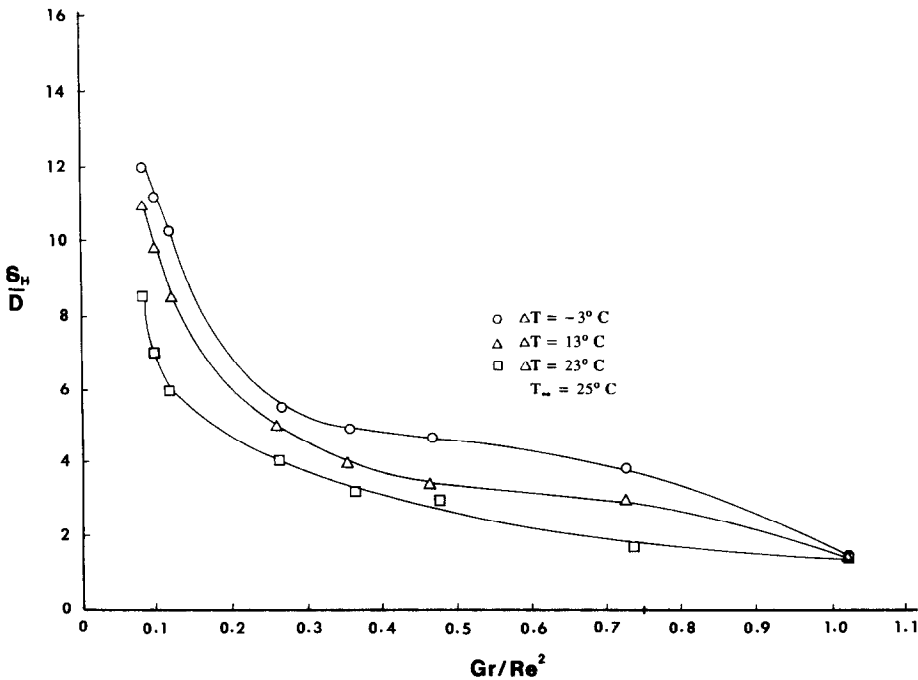


FIG. 8. Variation of the non-dimensional distance for heat loss  $\delta_H/D$  with  $Gr/Re^2$ .

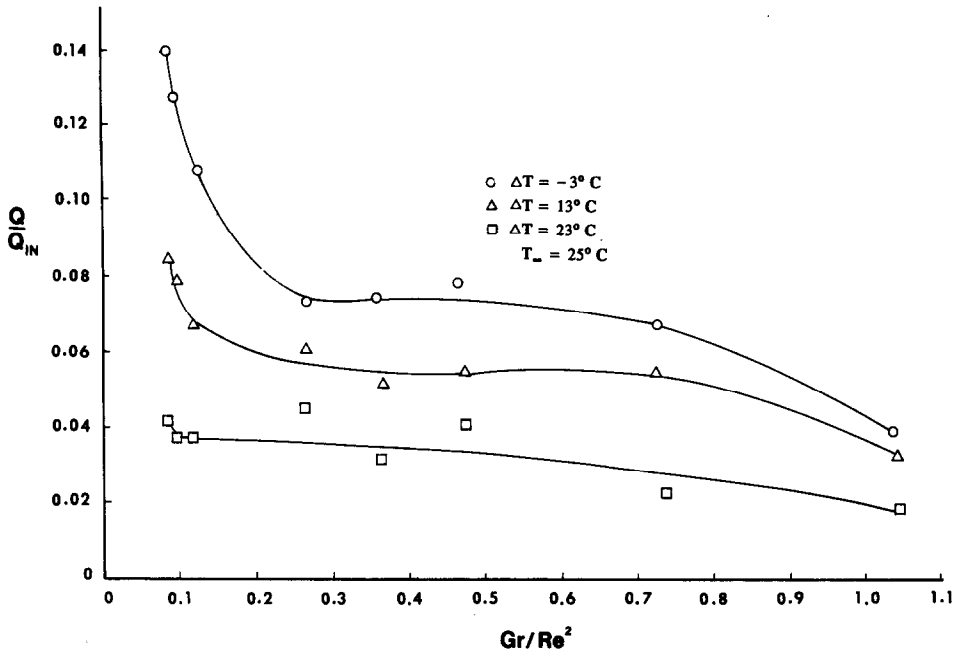


FIG. 9. Variation of the net energy lost to the plate by the jet  $Q$ , nondimensionalized by the total energy input  $Q_{IN}$ , with the mixed convection parameter  $Gr/Re^2$ .

Typically, 3–15% of the jet input energy is transferred to the plate. At large  $Gr/Re^2$ ,  $Q/Q_{IN}$  is found to be weakly dependent on  $Gr/Re^2$ , indicating that the penetration distance approaches an essentially constant value as  $Gr/Re^2$  increases to large values. This effect was also seen in Fig. 4.

The corresponding results in terms of the average Nusselt number  $\overline{Nu}_D = \bar{h}D/k$ , where  $\bar{h} = Q/W\delta_p\Delta T$  and  $W\delta_p$  is taken as the heat transfer area, are shown in Fig. 10. The trends are similar to those observed in

Fig. 9. It is interesting to note that the average Nusselt number  $\overline{Nu}_D$  tends to increase to large values as  $Gr/Re^2$  becomes small and to approach zero at large  $Gr/Re^2$ . The trends are clearly linked with the dependence of the penetration distance on  $Gr/Re^2$ . At small  $Gr/Re^2$ ,  $\delta_p$  is large and the jet loses much of its energy to the surface, whereas at large  $Gr/Re^2$ ,  $\delta_p$  is small and only a small portion of the jet energy is lost to the surface. Also, at a given  $Re$ , the inlet temperature  $T_0$  is lower at a smaller  $Gr/Re^2$ , resulting in a smaller

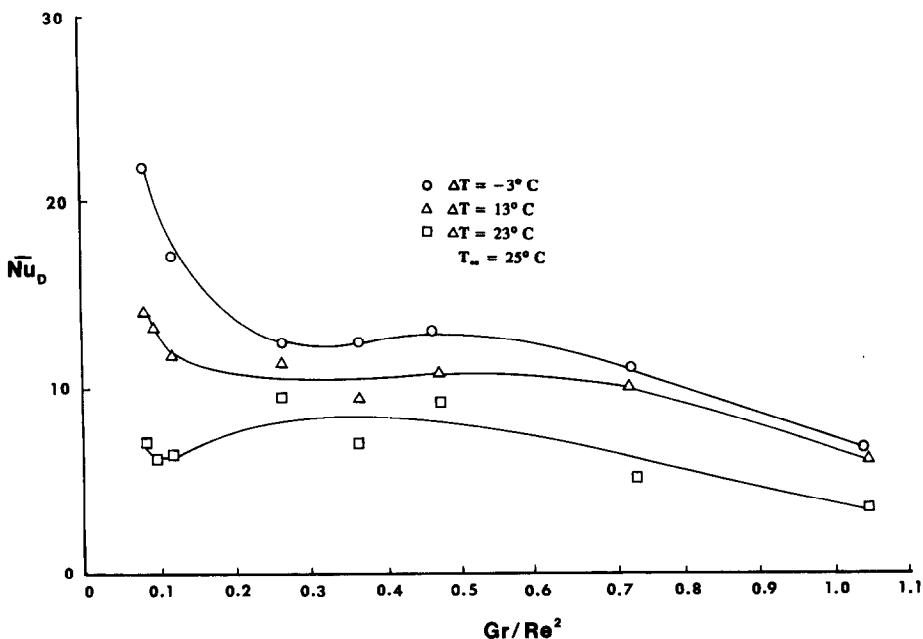


FIG. 10. Variation of the average Nusselt number  $\overline{Nu}_D$  with  $Gr/Re^2$ .

heat transfer rate to the surface. Thus, there are two competing effects. As  $Gr/Re^2$  becomes smaller, the area for heat transfer increases but the temperature difference ( $T_0 - T_s$ ) goes down. The combination of these opposing effects also gives rise to a maximum in  $\overline{Nu}_D$ , as seen in Fig. 10.

It may be mentioned that the net heat transfer  $Q$  up to  $x = \delta_p$  is considered here. However, only the heat lost by the jet  $Q_+$  may also be considered instead to obtain the heat transfer correlations. The transport process is complicated because of the presence of natural convection if  $T_s \neq T_\infty$  and the present approach attempts to focus on the transport process between the jet and the surface, avoiding a consideration of the natural convection transport. Presumably, the jet initially loses energy to the surface as the temperature in the flow approaches  $T_\infty$ . However, if  $T_s > T_\infty$ , the jet flow gains energy from the surface for some distance before flow reversal occurs. Beyond  $x = \delta_p$ , natural convection heat loss occurs. Similarly, if  $T_s < T_\infty$ , the surface gains energy from the environment by natural convection, which is absent only for  $T_s = T_\infty$ . This is clearly an interesting and complicated problem which needs a further detailed investigation.

An average Nusselt number  $\overline{Nu}_\delta$  based on the penetration distance  $\delta_p$  may also be defined as

$$\overline{Nu}_\delta = \frac{\bar{h}\delta_p}{k} = \frac{Q}{kW\Delta T} \quad (8)$$

since  $\bar{h} = Q/W\delta_p\Delta T$ . The variation of this average Nusselt number  $\overline{Nu}_\delta$  with  $Gr/Re^2$  can also be plotted for different wall conditions. It was again found that the Nusselt number decreases sharply up to around  $Gr/Re^2 < 0.2$ . This is then followed by a gradual decrease as  $Gr/Re^2$  increases. Since the effect of  $\delta_p$  on the Nusselt number is eliminated in this formulation, the variation of  $\overline{Nu}_\delta$  is similar to that of  $Q$ , as shown in Fig. 9.

The average Nusselt number  $\overline{Nu}_D$  varies with the wall temperature excess  $\Delta T$  and the mixed convection parameter  $Gr/Re^2$ , as shown in Fig. 10. Thus, a correlating equation may be derived from the data obtained to yield  $\overline{Nu}_D$  as a function of the dimensionless surface temperature excess  $\theta_s$  and  $Gr/Re^2$ . The result obtained is given as

$$\overline{Nu}_D = (10.3 - 13.4\theta_s)(Gr/Re^2)^{-(0.19 + 0.32\theta_s)} \quad (9)$$

This equation was found to provide a good representation of the data over the experimental ranges considered. A correlation coefficient of about 0.97 was computed, indicating the accuracy of this correlation.

## CONCLUSIONS

An experimental study has been carried out to investigate the heat transfer characteristics of a negatively buoyant, two-dimensional, wall jet. Negatively buoyant flows often arise in many problems of practical interest, such as enclosure fires, thermal discharge

into the environment and thermal energy storage systems. A heated, two-dimensional jet is discharged vertically downward adjacent to an isothermal surface in a large enclosure. A water cooled aluminum plate was employed and maintained at the desired wall temperature. The measurements consisted of the local heat flux distribution over the isothermal surface for various values of the mixed convection parameter  $Gr/Re^2$ , varying from 0.05 to 1.05. The thermal field in the flow was also measured in detail. The data were obtained for various wall temperatures.

The total heat transfer to the isothermal surface was determined by integrating the local heat flux  $q$  up to the jet penetration distance  $\delta_p$  along the surface. It was found that, typically, the total heat transfer to the surface  $Q$  decreases with an increase in  $Gr/Re^2$ . This is related to the decrease in jet penetration as  $Gr/Re^2$  is increased. It was also found that, with an increase in the wall temperature excess over the ambient,  $T_s - T_\infty$ , the total heat transfer from the jet to the surface,  $Q$ , decreases, as expected. The effect of wall temperature on jet penetration has also been investigated in detail. It is found that the jet penetrates to a shorter distance when the wall is kept at a temperature higher than that of the surroundings,  $\theta_s > 0$ , at a constant value of  $Gr/Re^2$ . This is attributed to the fact that, when the wall is warmer than the ambient, it induces a vertical upward, natural convection boundary layer flow adjacent to the wall. This flow opposes the jet which is discharged downward, resulting in a reduced penetration distance of the jet. Also the heat transfer reduced, resulting in larger opposing buoyancy effects.

**Acknowledgements**—This research was carried out with support from the Center for Fire Research of the National Bureau of Standards, United States Department of Commerce, Grant No. NB83-NADA4047. The several helpful suggestions of Dr L. Y. Cooper during the course of this work are also acknowledged.

## REFERENCES

1. C. J. Chen and W. A. Rodi, *Vertical Turbulent Buoyant Jets: a Review of Experimental Data*. Pergamon Press, Oxford (1979).
2. E. J. List, Turbulent jets and plumes, *Ann. Rev. Fluid Mech.* **14**, 189–212 (1982).
3. J. C. Mollendorf and B. Gebhart, Thermal buoyancy in round laminar vertical jets, *Int. J. Heat Mass Transfer* **16**, 735–745 (1973).
4. W. Schneider and K. Potsch, Weak buoyancy in laminar vertical jets. In *Review of the Developments in Theoretical and Experimental Fluid Mechanics* (Edited by U. Muller, K. G. Roesner and B. Schmidt). Springer, Berlin (1979).
5. Y. Jaluria, Hydrodynamics of laminar buoyant jets. In *Encyclopedia of Fluid Mechanics* (Edited by N. P. Cheremisinoff), Vol. 2, pp. 317–348. Gulf, Houston, Texas (1986).
6. L. Y. Cooper, On the significance of a wall effect in enclosures with growing fires, *Combust. Sci. Technol.* **40**, 19–39 (1984).
7. C. K. Cha and Y. Jaluria, Recirculating mixed convection flow for energy extraction, *Int. J. Heat Mass Transfer* **27**, 1801–1812 (1984).

8. J. S. Turner, Jets and plumes with negative or reversing buoyancy, *J. Fluid Mech.* **26**, 779–792 (1966).
9. R. A. Seban, M. M. Behnia and J. E. Abreu, Temperatures in a heated jet discharged downward, *Int. J. Heat Mass Transfer* **21**, 1453–1458 (1978).
10. Y. Jaluria, *Natural Convection Heat and Mass Transfer*, Chaps 3 and 4. Pergamon Press, Oxford (1980).
11. R. L. Alpert, Turbulent ceiling-jet induced by large scale fires, *Combust. Sci. Technol.* **11**, 197–213 (1975).
12. L. Y. Cooper, M. Harkleroad, J. Quintiere and W. Rinkinen, An experimental study of upper hot layer stratification in full-scale multiroom fire scenarios, *J. Heat Transfer* **104**, 741 (1982).
13. Y. Jaluria and K. D. Steckler, Wall flow due to fire in a room. *Proc. Fall Tech. Meeting*, Eastern Section of Combustion Institute, Atlantic City, New Jersey, Paper No. 47 (1982).
14. Y. Jaluria, Buoyancy driven wall flows due to enclosure fires. *Proc. 21st Symp. (Int.) Combust.*, Combustion Institute, Pittsburgh, Pennsylvania, pp. 151–157 (1986).
15. S. Satyanarayana and Y. Jaluria, A study of laminar buoyant jets discharged at an inclination to the vertical buoyancy force, *Int. J. Heat Mass Transfer* **25**, 1569–1577 (1982).
16. D. Goldman and Y. Jaluria, Effect of opposing buoyancy on the flow in free and wall jet, *J. Fluid Mech.* **166**, 41–56 (1986).
17. A. Roshko, On development of turbulent wakes from vortex street, NACA Tech. Rept. 1191 (1953).

### TRANSFERT THERMIQUE POUR UN JET PARIETAL NEGATIVEMENT FLOTTANT

**Résumé**—Une étude expérimentale est faite sur les caractéristiques du transfert thermique d'un jet pariétal, turbulent, bidimensionnel et flottant négativement. Le transfert thermique du jet vers la surface, avec une température de sortie du jet plus élevée que celle de la paroi, est mesuré en fonction de la distance le long de la surface isotherme, pour différentes valeurs des températures du jet et de l'ambiance. On trouve que le flux thermique transféré à la surface verticale isotherme décroît quand le paramètre de la convection mixte augmente. L'effet de l'écart de température de la surface sur la pénétration du jet vers le bas et sur le flux thermique transféré est étudié. On obtient des formules intéressantes.

### DER WÄRMEÜBERGANG AN EINEM DEM AUFTRIEB ENTGEGENGERICHTETEN WANDSTRAHL

**Zusammenfassung**—Es wurde eine experimentelle Untersuchung durchgeführt bezüglich der Wärmeübergangs-Eigenschaften eines turbulenten, abwärts gerichteten, zweidimensionalen Wandstrahls. Der örtliche Wärmeübergang vom Strahl an die isotherme Wandoberfläche wird entlang dieser Oberfläche für verschiedene Werte von Wand-, Strahl- und Umgebungstemperatur gemessen. Es wurde herausgefunden, daß der Gesamt-Wärmeübergang an der isothermen vertikalen Oberfläche mit zunehmendem Misch-Konvektionsparameter kleiner wird. Der Einfluß der Temperaturdifferenz zwischen Strahl und Wand auf die abwärtsgerichtete Strahlänge und auf das Wärmeübertragungsvermögen wurde ebenfalls untersucht. Korrelations-Gleichungen werden abgeleitet.

### ТЕПЛОПЕРЕНОС ОТ ПРИСТЕННОЙ СТРУИ С ОТРИЦАТЕЛЬНОЙ ПЛАВУЧЕСТЬЮ

**Аннотация**—Экспериментально исследуются характеристики теплопереноса турбулентной двумерной пристенной струи с отрицательной плавучестью. Теплоперенос к поверхности от струи, температура которой при истечении превышает температуру поверхности, рассматривается как функция расстояния вдоль изотермической поверхности для нескольких значений температуры стенки, струи и окружающей среды. Найдено, что суммарная интенсивность теплопереноса к изотермической вертикальной поверхности уменьшается с увеличением коэффициента смешанной конвекции. Изучено также влияние избыточной температуры поверхности на распространение струи вниз и на интенсивность теплопереноса. Выведены соответствующие корреляционные зависимости.